SUPPLEMENTARY METHODS

RT-PCR. RNA was isolated using a PureLink RNA Mini Kit (Ambion, Grand Island, NY) and treated with TURBO DNA-free (Ambion) to remove genomic DNA. First-strand cDNA was synthesized using a SuperScript VILO Master Mix (Invitrogen). RT-PCR was performed using Taqman Gene Expression Assays (list follows) and TaqMan Universal PCR Master Mix, No AmpErase UNG (Applied Biosystems) per manufacturer's protocol.

Taqman Gene Expression Assays:

iPS Cell Markers

GAPDH Hs 99999905_m1

POU5F1 Hs 00999634_gH

SOX2 Hs 00602736_s1

NANOG Hs 02387400_g1

KLF4 Hs 00358836_m1

MYC Hs 00153408_m1

LIN28 Hs 00702808_s1

REX01 Hs 00810654_m1

ABCG2 Hs 01053790_m1

DNMT3 Hs 01003405_m1

Skin Markers

Col7a1 HS 01574733_g1

Col17 HS 00166711_m1

Krt1 HS 00196158_m1

Krt5 HS 00361185_m1

Krt15 HS 00267035_m1

Endogenous-versus-total RT-PCR. RNA was isolated using a PureLink RNA Mini Kit (Ambion) and treated with TURBO DNA-free (Ambion) to remove genomic DNA. First-strand cDNA was synthesized using a SuperScript VILO Master Mix (Invitrogen). RT-PCR was performed using an ABI 7500 Real Time PCR System and Power SYBR Green (Applied Biosystems). The following primer sets were used:

beta-Actin Forward TGAAGTGTGACGTGGACATC

beta-Actin Reverse GGAGGAGCAATGATCTTGAT

OCT4 Endo Forward CCTCACTTCACTGCACTGTA

OCT4 Endo Reverse CAGGTTTTCTTTCCCTAGCT

OCT4 Total Forward	AGCGAACCAGTATCGAGAAC
OCT4 Total Reverse	TTACAGAACCACACTCGGAC
SOX2 Endo Forward	CCCAGCAGACTTCACATGT
SOX2 Endo Reverse	CCTCCCATTTCCCTCGTTTT
SOX2 Total Forward	AGCTACAGCATGATGCAGGA
SOX2 Total Reverse	GGTCATGGAGTTGTACTGCA

Bisulfite genomic sequencing. Genomic DNA was isolated using a PureLink Genomic DNA Mini Kit (Invitrogen). Bisulfite treatment was done using an EpiTect Bisulfite kit (Qiagen, Alameda, CA). Converted DNA was PCR-amplified using OCT4 primer sets 2,4 and NANOG primer set. PCR products were gel purified using a PureLink Quick Gel Extraction and PCR Purification Combo Kit (Invitrogen) and cloned into bacteria using the TOPO TA Cloning Kit for Sequencing (Invitrogen).

SUPPLEMENTARY FIGURES

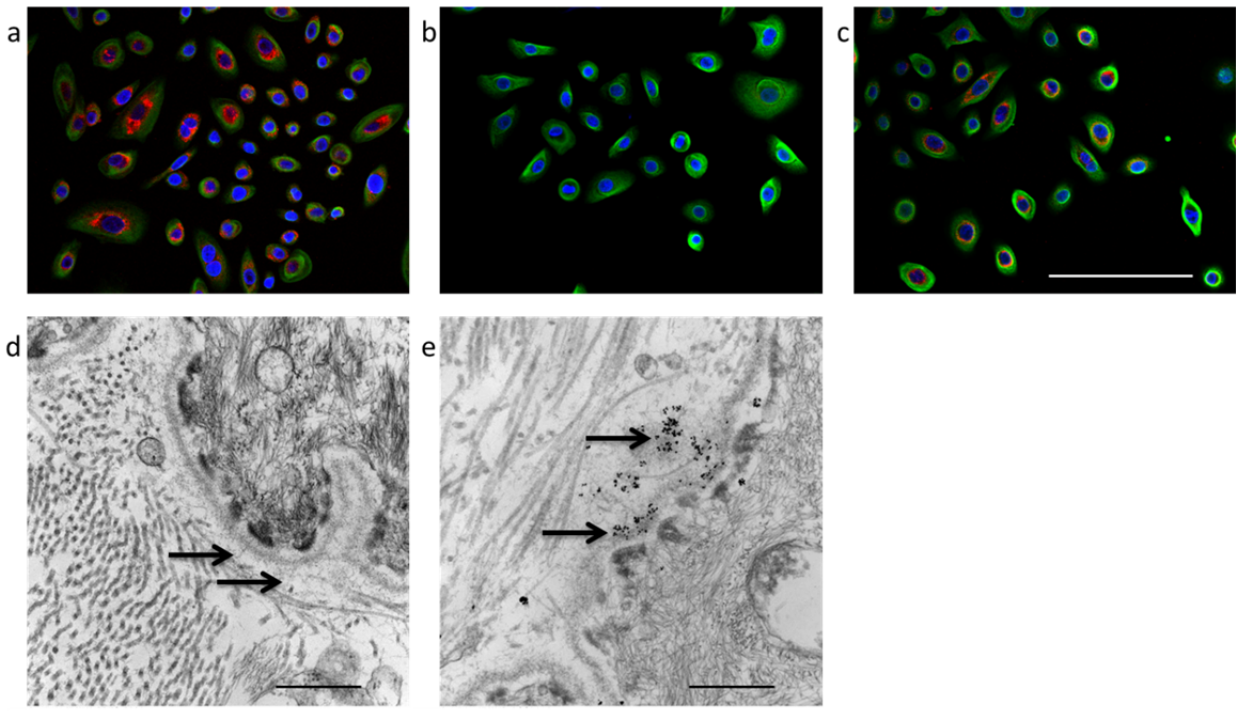

Supplementary Figure 1. Type VII collagen expression in revertant keratinocytes and skin. (a-c) Keratinocytes derived from non-blistered skin (left panel), mutant skin (middle panel,) and wild-type skin (right panel) stained with antibodies to type VII collagen (red) and keratin 5 (green). Nuclei are stained with DAPI (blue). (d) Ultrastructural examination of non-blistered skin shows narrow, sometimes looping anchoring fibrils extending from the basal lamina into the dermis (arrows). (e) Immunolabeling of same sections shows type VII collagen localized to the dermal-epidermal junction at the lamina densa and fibrilllar structures just below the lamina densa. Immunogold deposits are most concentrated subjacent to hemidesmosomes. Scale bar = 50 µm.

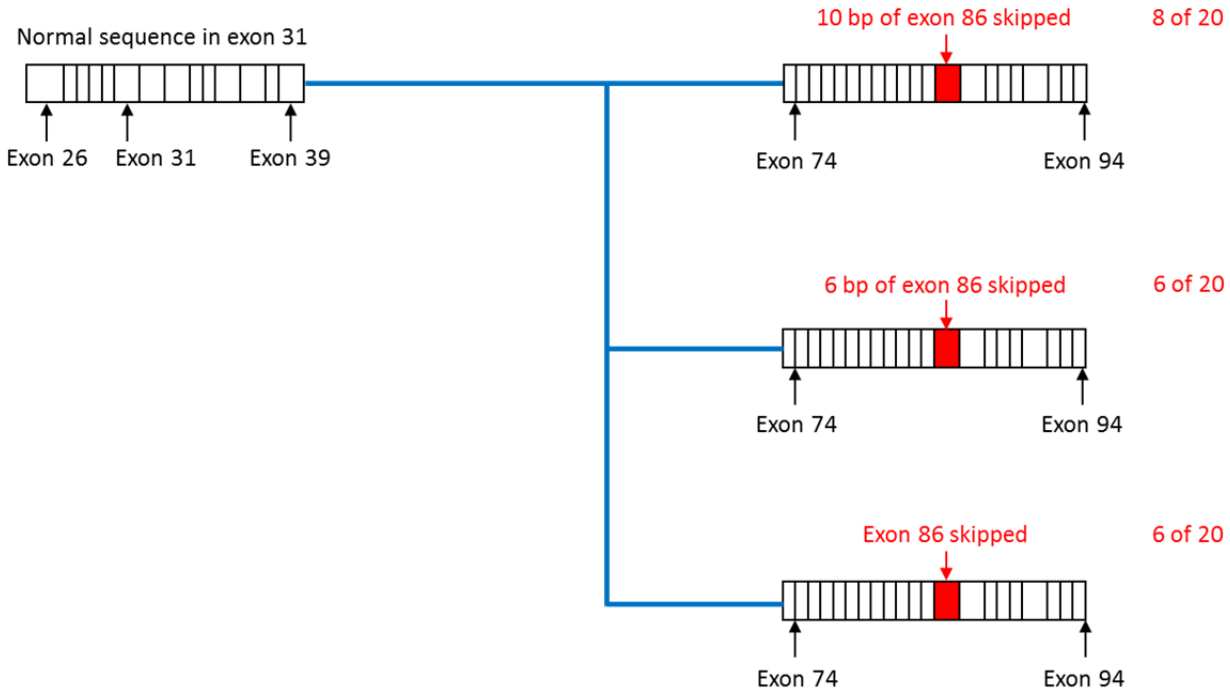

Supplementary Figure 2. Pathomechanism of *COL7A1* reversion in non-blistered skin. To assess the molecular events surrounding the paternal frameshift mutation c.3840delC and maternal acceptor splice site mutation g.6751-2A>G, following reverse transcription, cDNA was PCR amplified using primers complementary to sequences in exon 26 and exon 94. Two bands were observed approximately 1,500 base pairs (bp) apart. Cloning and sequencing of the smaller band (approximately 2,250 bp) revealed that all colonies (N=28) harbored mutation c.3840delC. Cloning and sequencing of the larger band (approximately 3,720 bp) revealed that minority of colonies (8 of 28) also harbored mutation c.3840delC, but the rest (20 of 28 colonies) did not. In these 20 samples, three downstream variants were observed: skipping of first 10 bp of exon 86 (N=8), skipping of first 6 bp of exon 86 (N=6), and skipping of the whole exon 86 (N=6). As in the latter two variants (N=12), the *COL7A1* sequence remains in-frame. We conclude that this is the pathomechanical molecular correlate to the C7 protein expression in mosaic skin sections (**Figure 1d**) and keratinocytes cultured from it (**Supplementary Figure 1**), to ultrastructural analysis revealing anchoring fibrils (**Supplementary Figure 1d and 1e**), and to clinical observation of the skin patch with normal-appearing skin (**Figure 1a and 1b**).

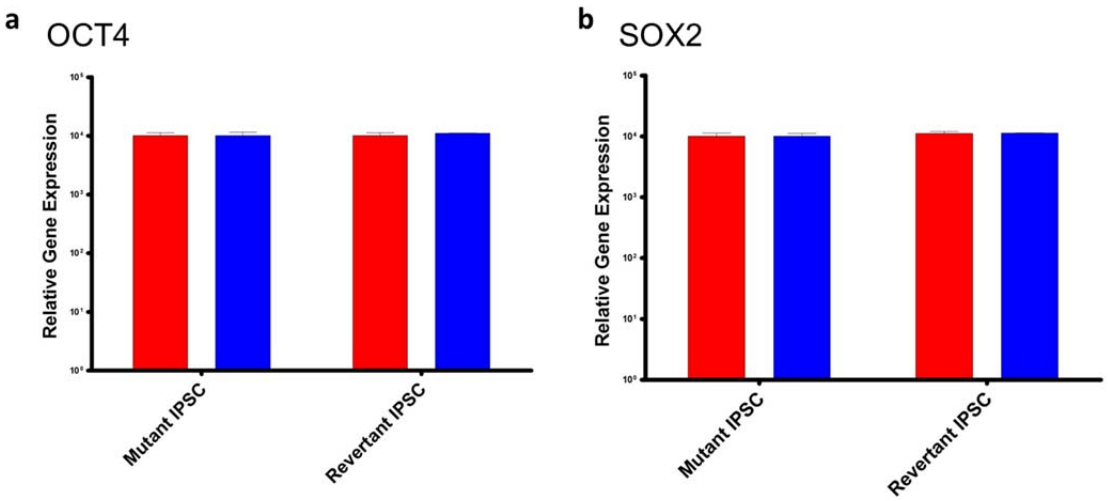

Supplementary Figure 3. Exogenous reprogramming genes are silenced in iPSCs. (a) Expression of *OCT4* gene. (b) Expression of *SOX2* gene. Endogenous levels of expression (red bars) and the total levels of expression (blue bars) in mutant and revertant iPSCs are not statistically different, confirming the silencing of exogenously provided reprogramming genes. Of note, the simultaneous silencing of the exogenous reprograming genes and new expression of their endogenous counterparts defines fully reprogrammed iPSCs.

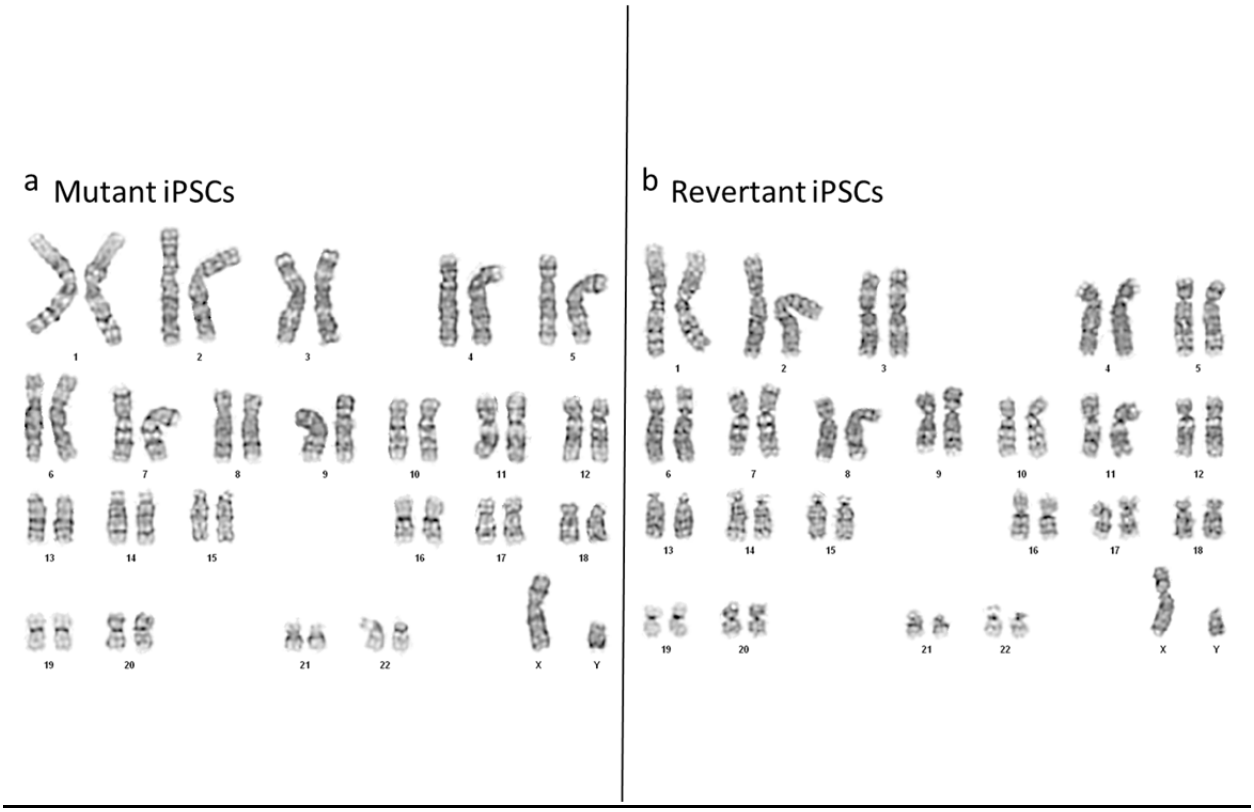

Supplementary Figure 4. Cytogenetic analysis of iPSCs. (a) Normal karyotype of iPSCs derived from blistered skin (mutant iPSCs). (b) Normal karyotype of iPSCs derived from non-blistered skin (revertant iPSCs).